Enzymatically crosslinked hydrogel based on tyramine modified gelatin and sialylated chitosan

Peng Ding[1,2,*], Qianqian Wei[1], Ning Tian[1], Xiaoyue Ding[1], Ling Wang[1], Bin Wang[1], Oseweuba Valentine Okoro[3], Amin Shavandi[3,*], and Lei Nie[1,3,*]

[1] School of Life Science, Xinyang Normal University, Xinyang464000, China

[2] Tea Plant Biology Key Laboratory of Henan Province, Xinyang 464000, China

[3] 3BIO-BioMatter, Avenue F.D. Roosevelt, 50 - CP 165/61, 1050 Brussels, Belgium

*** Corresponding author**

Dr. Lei Nie

Post address: College of Life Sciences, Xinyang Normal University (XYNU), Xinyang 464000, China. Tel: +86-13600621068. ORCID: 0000-0002-6175-5883

E-mail address: nieleifu@yahoo.com; nielei@xynu.edu.cn

Dr. Peng Ding

Post address: College of Life Sciences, Xinyang Normal University (XYNU), Xinyang 464000, China.

E-mail address: dingzhiyu120@163.com

Dr. Amin Shavandi

Post address: BioMatter unit - École polytechnique de Bruxelles, Université Libre de Bruxelles, Avenue F.D. Roosevelt, 50 - CP 165/61, 1050 Brussels, Belgium

E-mail address: amin.shavandi@ulb.be

Abstract

The enzymatically crosslinked hydrogel could replicate the cellular microenvironment for biomedical applications. In the present study, to improve the cytocompatibility of chitosan (CS), sialic acid (SA) was introduced to CS to synthesize sialylated CS (CS-SA), and the tyramine (TA) was grafted to gelatin (G) to obtain TA modified gelatin (G-TA). The successful synthesis of CS-SA and G-TA was confirmed using ^{1}H NMR and UV-Vis absorption spectra. The interpenetrating polymer networks (IPN) G-TA/CS-SA (GC) hydrogel (GC) was then fabricated via blending G-TA and CS-SA solutions and crosslinked using horseradish peroxidase (HRP). The storage modulus (G') of the fabricated GC hydrogels with different ratios of G-TA/CS-SA greatly varied during the formation and strain of hydrogels. With the increase of CS-SA concentration from 0 % to 2 %, the storage modulus of GC hydrogels was also observed to decrease from 1500 Pa to 101 Pa; the water uptake capacity of GC hydrogels increased from 1000 % to 4500 %. Additionally, the cell counting kit-8 (CCK-8) and fluorescent images demonstrated the excellent cytocompatibility of GC hydrogels after culturing with NIH 3T3 cells. The obtained results indicated that the fabricated GC hydrogels might have potential in biomedical fields, such as wound healing dressing.

Keywords: chitosan; sialic acid; tyramine; gelatin; hydrogel

1. Introduction

Hydrogels crosslinked with hydrophilic polymer networks are widely considered promising materials for tissue engineering and regenerative medicine [1-3]. The hydrated structure of hydrogels facilitates oxygen and nutrient transfer for the creation of a peripheral environment that is similar to the native extracellular matrix and thus promotes cell proliferation, differentiation, and gene expression [4-7]. Different natural polymers such as fibrin, alginate, collagen, hyaluronic acid, gelatin and chitosan have been investigated as functional biomaterials for hydrogel production, with gelatin considered particularly promising. This is because gelatin constitutes the main extracellular component of connective tissues, including cartilage, bone and skin [4, 6, 8-14] and is rich in arginine-glycine-aspartic (RGD) peptide sequence. The abundance of the RGD peptide sequence enabled gelatin's integration with hyaluronic acid, poly(ethylene glycol), alginate and silk fibroin to improve their bioactivity for skin [15-24], cartilage [12, 13, 25-30] and nerve tissue engineering applications [31, 32]. Chitosan is another natural polymer that has been used for biomedical materials due to its biodegradability, anti-infection activity, biocompatibility and hemostatic activity, although its applicability is limited by its poor solubility in aqueous solution [33]. Chitosan possesses many reactive functional hydroxyl and amino/acetamido groups that facilitate diverse chemical modifications to produce various chitosan-based hydrogels for various biological applications [6, 20, 22, 34].

It is acknowledged that stereospecific saccharide-saccharide interactions at the cell surface perform essential roles in various cellular processes, such as cell adhesion,

signalling and recognition [35-40]. For instance, oligosaccharide Lewis (X)-Lewis (X) interaction induces cell adhesion in embryonic development [41], and dissociated sponge cells from two different species can reaggregate through surface proteoglycans in a Ca^{2+}-rich environment by sorting out according to their species of origin [42]. Moreover, in previous articles, mono- or di-saccharide groups were creatively introduced into a polymeric interface material to enhance the affinity to glycopeptides based on saccharide-saccharide interactions [43-45]. These examples inspire an investigation into the introduction of a saccharide group such as sialic acid to a hydrogel surface to potentially enhance interaction between cells and materials for enhanced cell biocompatibility of materials.

In addition, the interpenetrating polymer networks (IPN) hydrogels using the combination of two or more topologically interlocking polymer chains could readily achieve favourable mechanical properties and recapitulate complex cell-matrix interactions [46]. This study had therefore sought to investigate the modification of chitosan with sialic acid (N-acetylneuraminic acid) (CS-SA) and the functionalization of gelatin with tyramine (G-TA) to produce IPN hydrogels. The *in situ* forming IPN GC hydrogels will be developed using the enzymatic oxidative reaction of HRP and H_2O_2 [47], (**Figure 1)** and the physicochemical properties and cytocompatibility of the prepared IPN GC hydrogels subsequently evaluated.

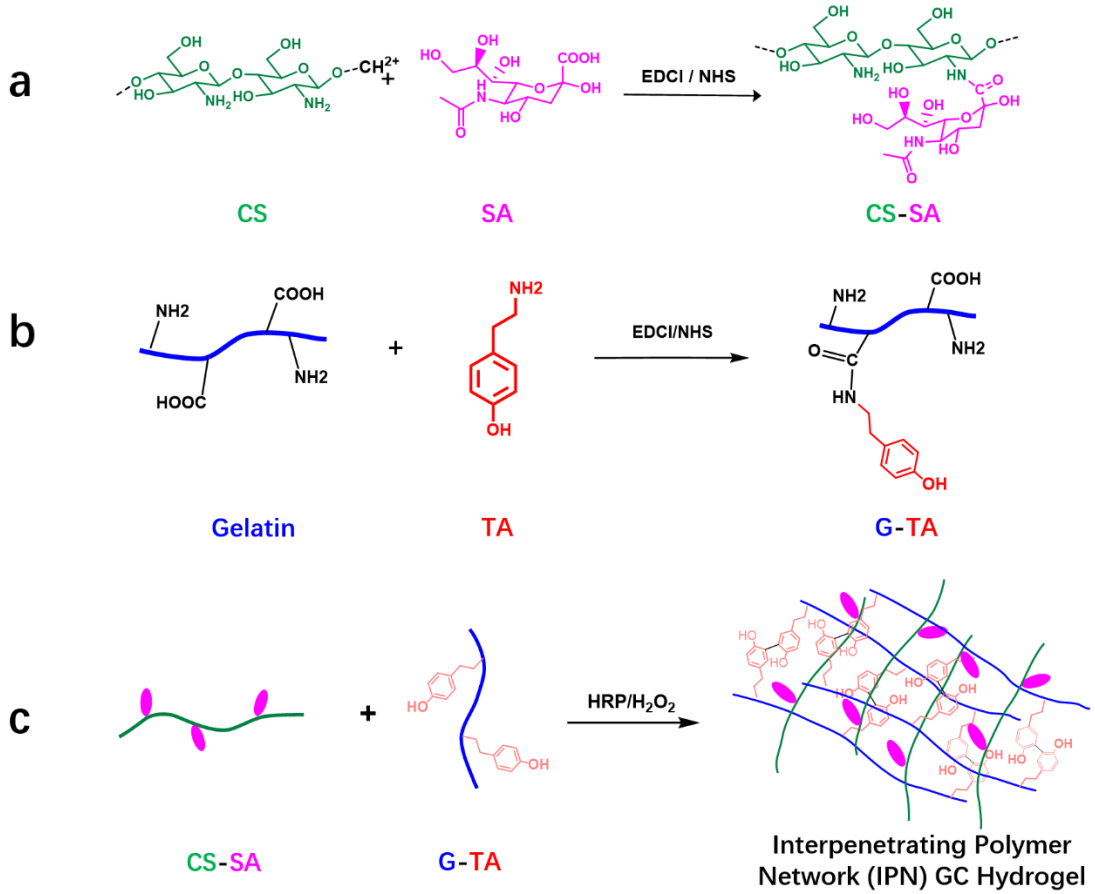

Figure 1. Schematic representation of IPN GC hydrogel by an enzyme-catalysed oxidation reaction. (a) Synthesis of sialic acid grafted chitosan (CS-SA). (b) Carbodiimide coupling of tyramine (TA) to carboxylic acid residues on gelatin. (c) HRP-mediated covalent crosslinking of G-TA and the formation of IPN GC hydrogels.

2. Experimental section

2.1 Materials

Chitosan (CS, SKU: 448855, degree of deacetylation: 75-85%, medium molecular weight, viscosity: 200 – 800 cP), Sialic acid (SA), 3-(4-hydroxyphenyl) propionic acid (HPA), N-hydroxysuccinimide (NHS), morpholinoethanesulfonic acid (MES), 1-ethy-3-(3-dimethylaminopropyl carbodiimide) hydrochloride (EDC·HCl, EDCI) and

horseradish peroxidase (HRP, 300 IU/mg) were purchased from Aladdin Co., Ltd (Shanghai, China). Gelatin type A (SKU: 924504-IEA, powder) was purchased from Merck Co., Ltd. Dimethylformamide (DMF) and hydrogen peroxide (H_2O_2) were bought from Sinopharm Chemical Reagent Co., Ltd. All chemicals and solvents purchased were used as received without further purification.

2.2 Synthesis of sialylated chitosan (CS-SA)

Briefly, chitosan (1.2 g) was fully dissolved in 200 mL of 1 wt% acetic acid aqueous solution, followed by pH adjustment to 6 using 5 M NaOH. Sialic acid (2.0 g), EDCI (3.7 g), and NHS (1.7 g), were dissolved in a 0.1 M MES buffer solution (50 mL) and stirred for 30 min and subsequently added to the chitosan solution [48]. The solution was stirred (500 rpm) at 22 ^{o}C for 12 h, with the resulting sialylated chitosan product subsequently dialyzed against Millipore water using a 7000 Da molecular weight cutoff dialysis membrane for 3 days, followed by lyophilization.

2.3 Synthesis of gelatin conjugates (G-TA)

Gelatin (2.5 g) was dissolved in 100 mL of Millipore water at 60 ^{o}C and stirred for 1 h to facilitate complete dissolution. NHS (15 mg) and EDCI (25 mg) were added to HPA (20 mmol) and dissolved in 100 mL of a co-solvent of DMF and water (volume ratio of 2:3). Then, the activated HPA solution was transferred to the gelatin solution, and the mixture reacted at 40 ^{o}C for 12 h. Finally, the resulting solution was dialyzed against Millipore water for 3 days and subsequently lyophilized to facilitate product recovery [2].

2.4 Preparation of enzymatically crosslinked IPN GC hydrogels

After a couple of pre-experiments to prepare GC hydrogels, the following method was used to fabricate GC hydrogels. The prepared G-TA was dissolved in phosphate buffer (pH at 7.4), and then the CS-SA was added to the G-TA solution to obtain G-TA/CS-SA composite solution. 10 μL of H_2O_2 solution (167 mM) and 10 μL of HRP solution (1000 U/mL) were added to each tube, and 1 mL of G-TA/CS-SA composite solution was added respectively. Then the IPN GC hydrogel was formed after a composite of two solutions with gentle stirring. The nomenclature of the as-prepared GC hydrogels is expressed as follows: X-C-Y, where X represents the concentration of G-TA and Y represents the concentration of CS-SA. In this work, 5C0, 5C1, 5C2, 8C0, 8C1, and 8C2 were prepared.

2.5 ^{1}H NMR analysis

A proton nuclear magnetic resonance (^{1}H NMR) spectrometer was used to investigate the chemical composition of CS, SA, CS-SA, gelatin, and G-TA. The polymers were dissolved in deuterium oxide (D_2O), and ^{1}H NMR measurements were performed on a 600 MHz NMR spectrometer (ECZ600R/S3, JEOL RESONANCE Inc., Japan) equipped with a 14.09 T superconducting magnet and a 5.0 mm 600MHz broadband Z-gradient high-resolution ROYAL probe.

2.6 UV-Vis analysis

The UV-Vis spectra of gelatin and G-TA were tested using Ultraviolet-visible spectroscopy (UV-Vis, PerkinElmer Lambda 950, USA). The samples were dissolved in distilled water at 0.1% (w/w), and the introduced phenolic hydroxyl (Ph) groups in G-TA were confirmed by detecting the absorbance at 275 nm.

2.7 Rheology analysis

Rheological measurement of the prepared GC hydrogels was performed using a rheometer (TA, DHR, USA) equipped with a 20 mm stainless steel upper cone and temperature-controlled Peltier bottom plate, at 37 ºC [49]. Briefly, a 420 µL aliquot of pre-hydrogel solutions with 2.5 U/mL HRP was loaded to the Peltier, and the cone was lowered to a specified gap. Low viscosity oil was placed around the outside edge of the cone to prevent water evaporation. Meanwhile, 4.2 µL of 0.5 vol.% H_2O_2 was injected into the gap to initiate the gelation. A dynamic time sweep was conducted at 1 Hz with 1% applied strain for 4000 s to determine gelation kinetics and storage moduli. Following gelation, dynamic frequency sweeps (0.1-100 rad/s at 1 % strain) and strain sweeps (0.1 % - 500 % or to failure, at 1 Hz) were performed to analyze the elastic behaviour of the resulting hydrogels.

2.8 Water uptake analysis

The water uptake of the prepared GC hydrogels was measured using a gravimetric method at 22 ºC. Briefly, the as-prepared cylindrical hydrogel samples were fully immersed in PBS buffer at 22 ºC . The swollen samples were weighed at specific time intervals until they reached swelling equilibrium. Then, the hydrogels were freeze-dried until a constant weight was obtained. The water uptake (WU) of the hydrogels in PBS buffer was then calculated as follows;

$$WU = \frac{W_s - W_d}{W_d} \quad (1)$$

Where W_s is the mass in g of the swollen hydrogel sample and W_d is the dry mass in g of the hydrogel sample.

2.8 SEM analysis

The morphology of the cross-section of GC hydrogels was characterized by SEM. The lyophilized as-prepared GC hydrogels were immersed in liquid nitrogen for rapid freezing. The samples were then cut off using a sharp blade. The cut cross-sections were then sprayed with platinum for 40 s, and the morphology was subsequently observed using a cold field emission scanning electron microscopy (SEM, Hitachi, S-4800) with an accelerating voltage of 10 kV imposed.

2.10 Cell counting kit-8 (CCK-8) analysis

The cytocompatibility of the GC hydrogels was conducted by evaluating the viability of NIH 3T3 cells cultured with the GC hydrogels. CCK-8 was used to investigate the viability of NIH 3T3 cells after seeding on GC hydrogels and culturing for different days, the O.D value at 450 nm was measured to indicate the presence of metabolically active NIH 3T3 cells, and cells cultured without hydrogels as a control group [8]. The NIH 3TS cells (CRL-1658^{TM}, ATCC) were grown in Dulbecco's modified Eagle's medium (DMEM) with 10 % fetal bovine serum, 100 U mL^{-1} penicillin, and 100 μg mL^{-1} streptomycin under a humidified atmosphere of 5 % CO_2 and 95 % air at 37 ºC, according to ATCC instruction. Cells at passage 5 for the next experiments. The prepared GC hydrogels were soaked in 75 % of alcohol overnight and replaced by PBS on the ultra-clean working table. All hydrogels were added to a 48-well plate (Corning), and 1 mL of NIH 3TS cells solution was added to each well (1×10^4 cells/mL), and incubated at 37 ºC in a 5 % CO_2 atmosphere, using the culture medium as a control. After incubating for 1 day, 2 days, and 3 days, the samples were

treated with CCK-8 kit solution (10 μL), and then incubated for 2 h at 37 ºC. Finally, the reaction solutions were transferred to a 96-well plate. The optical density (O.D) at 450 nm for each well was tested using a microplate reader (Tecan GENios, Tecan Austria GmbH, Salzburg, Austria).

2.11 Fluorescent microscopy analysis

The phalloidin-FTTC and 4'6-diamidino-2-phenylindole (DAPI) were used to stain the cells seeded in the prepared GC hydrogels. The procedure was described in our previous report [11]. Briefly, the hydrogels were cultured with NIH 3TS cells for 3 days, the hydrogels were washed using PBS and fixed with 2 % glutaraldehyde for 10 min. Then the hydrogels were washed with PBS and treated using 0.1 % of Triton X-100, then phalloidin-FITC and DAPI were subsequently used. Finally, the treated hydrogels were washed using PBS again, and the fluorescent microscopy images were obtained using a confocal laser scanning microscope (CLSM, Leica TCS SP5 II, Germany).

2.12 Statistical analysis

All experiments were conducted in triplicate, and the data were expressed as means with standard deviation. The SPSS software (SPSS Inc, Chicago IL) was used for the analysis. ANOVA statistical analyses and Tukey's test were applied to investigate specific differences between the control group and tested group for CCK-8 results. Statistical significance was defined at a p-value of < 0.05 and < 0.01 for 95% and 99% confidence, respectively.

3. Results and discussion

3.1 Synthesis and characterization of CS-SA and G-TA

Chitosan is an insoluble nature polymer in neutral aqueous solutions [50]. In this work, the chitosan was modified by reacting sialic acid (SA) with primary amino groups of chitosan through EDCI/NHS activation to improve its water solubility (**Fig. 1a**). The successful synthesis of CS-SA was evaluated using the ^{1}H NMR spectra analysis (**Fig. 2a**). As shown in the spectrum of CS-SA, chemical shifts at 2.99, 3.48-3.74 ppm were assigned to the hydrogen protons of [H1] and [H2]-[H5], respectively. As for the ^{1}H NMR spectrum of SA, peaks at 1.77, 1.88, 3.38, 3.44, 3.58 and 3.66 ppm were assigned to the hydrogen protons of [H6], [H9], [H7], [H11], [H10], [H8], respectively. However, the ^{1}H NMR spectrum signal of the raw chitosan did not initially have the above peaks, with the peaks becoming visible when in the ^{1}H NMR spectrum signal of the CS-SA conjugate, confirming the successful graft of SA to chitosan. The successful introduction of Ph groups was confirmed using UV-Vis spectrum analysis with the UV-Vis spectra of G and G-TA displayed in **Fig. 2b**. The detection of absorbance at a peak 275 nm in the UV-Vis spectrum confirmed the successful synthesis of G-TA. Such a result could also be confirmed using ^{1}H NMR analysis (**Fig. 2c**). The ^{1}H NMR spectrum of G-TA clearly showed that the integration value corresponding to phenol groups (6.5-7.2 ppm) was much higher than that of gelatin, indicating the conjugation of TA to gelatin backbones.

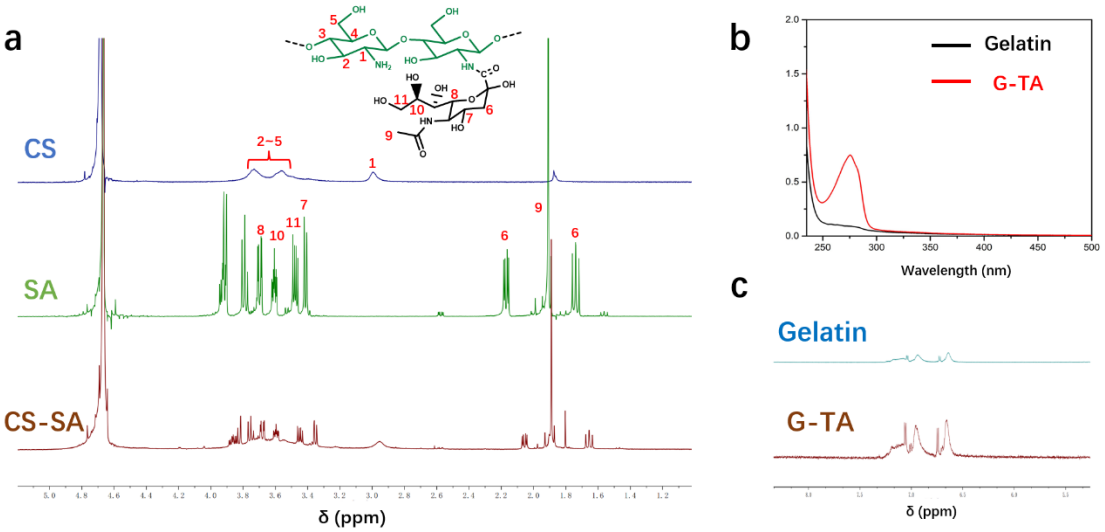

Figure 2. (a) ^{1}H NMR spectra (D_2O) of CS, SA and CS-SA, (b) UV-Vis spectra of gelatin and G-TA, (c) ^{1}H NMR spectra (D_2O) of gelatin and G-TA.

3.2 Rheological analysis and water uptake of GC hydrogels

The GC hydrogel could be obtained by mixing G-TA/CS-SA/H_2O_2 and G-TA/CS-SA/HRP solutions with gentle shaking, and the formation of GC hydrogel could be evaluated by a tube inversion method (**Fig. 3a**) [51, 52]. The prepared GC hydrogels could be injected using a syringe, and the filament was obtained, confirming the injectability of GC hydrogels (**Fig. 3b**) [53]. Next, the kinetics of gelation and mechanical properties of the prepared GC hydrogels were assessed using oscillatory rheology experiments (**Fig. 3c** and **3d**). The GC hydrogels of varying CS-SA and G-TA concentrations containing HRP and H_2O_2 were *in situ* formed in a cone and plate geometry, maintained at 37 ^{o}C. **Fig. 3c** displayed that all the samples with mixing the polymer solutions increased the storage modulus (G') due to enzymatically crosslinked reactions of G-TA, until a plateau value was attained, indicating a plateau value at the end of the crosslinking process. It was observed that a higher G-TA concentration

resulted in a higher storage modulus, while the storage modulus decreased as the CS-SA content increased. In addition, the linear viscoelastic region was also conducted by the strain amplitude sweep at a range of 0.1-500% at 1 Hz (**Fig. 3d**), with the storage modulus of all the prepared GC hydrogels shown to remain constant in a wide range of strain. This observation indicated that the GC hydrogels had a highly stable structure under a relatively high degree of deformations. Notably, however, the storage modulus was observed to decrease with an increase in CS-SA content. For the prepared GC hydrogels, the simultaneous IPN would be formed after mixing G-TA/CS-SA/H_2O_2 and G-TA/CS-SA/HRP solutions, CS-SA polymer chains spread in both solutions, and then the G-TA polymer network formed with the enzymatic oxidative reaction of HRP and H_2O_2 (**Fig. 1c**) [46, 47, 54].

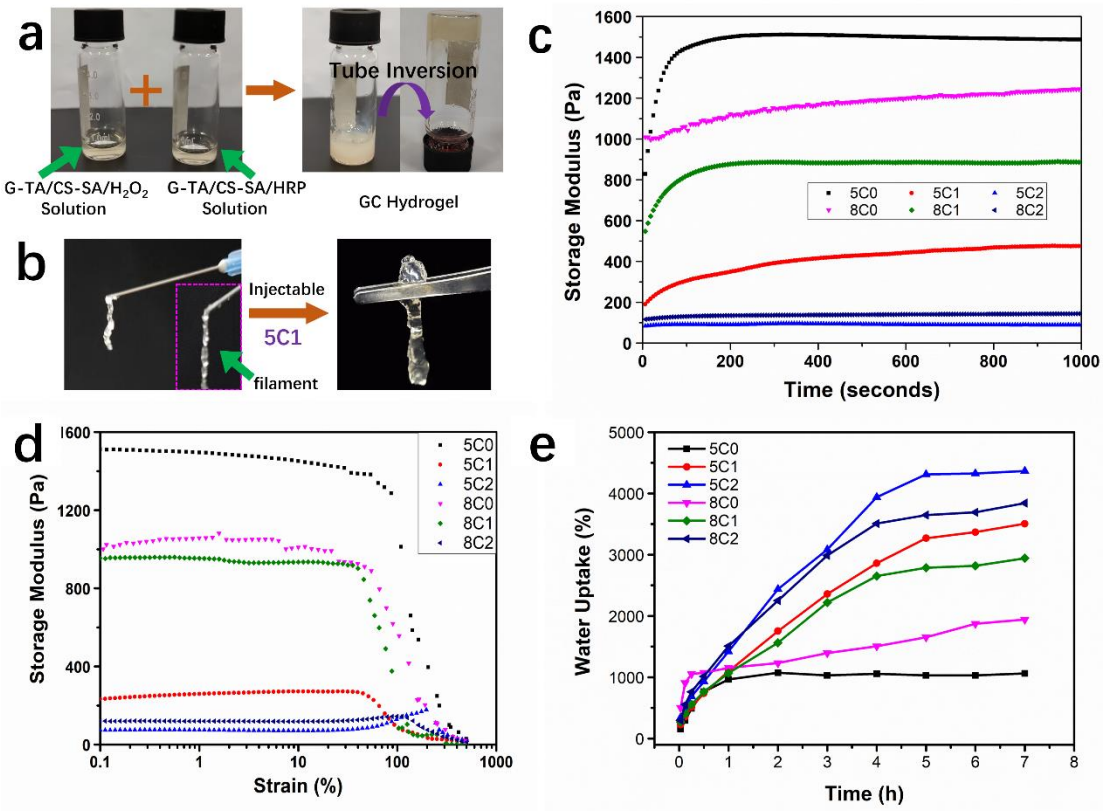

Figure. 3 (a) The HRP/H_2O_2 mediated *in situ* formed GC hydrogel could be prepared by

compositing G-TA/CS-SA/H_2O_2 and G-TA/CS-SA/HRP solutions, the hydrogel formation was identified using the tube inversion method. (b) The GC hydrogel (5C1) could be injected using a syringe, and the filament was formed. Rheological properties of GC hydrogels, (c) representative time sweeps, (d) strain sweeps. (e) Water uptake capacity of GC hydrogels.

The water uptake capacity is an essential feature of the hydrogels because it relates to other properties, including their mechanical properties and pore size, which further influences the nutrient transport, drug delivery and tissue exudate adsorption through hydrogels [55]. **Fig. 3e**. shows that the water uptake capacity of GC hydrogels increased from 1000 % to 4500 % as the CS-SA concentration increased from 0 % to 2 %. This observation was due to the improved hydrophilicity of CS-SA after grafting SA to CS. It was also noticed that the sample 5C2 hydrogel with the highest CS-SA concentration displayed the highest water uptake capacity, which increased to 4300 % after 7 h, compared to other samples. The water uptake capacity of GC hydrogels was also influenced by the G-TA content, which due to that, the enzymatically crosslink degree increased with the increase of G-TA concentration.

3.3 Microstructure of GC hydrogels

The microstructure of the cross-section of the as-prepared GC hydrogels (**Fig. 4)** showed a 3D, relatively homogeneous, and interconnected pore structure, which indicated good structural stability and uniform chemical structure for all prepared GC hydrogels. The porous interconnected structure provides enough space for cell growth, attachment, proliferation, and extracellular matrix secretion [13, 21, 56].

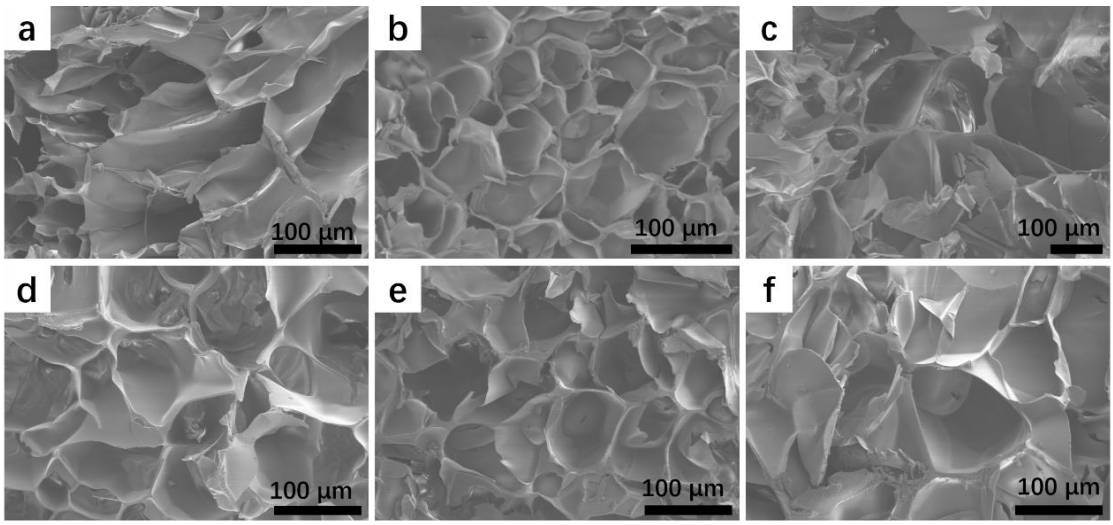

Figure 4. SEM images of the prepared GC hydrogels after freezed-dried, (a) 5C0, (b) 5C1, (c) 5C2, (d) 8C0, (e) 8C1, and (f) 8C2.

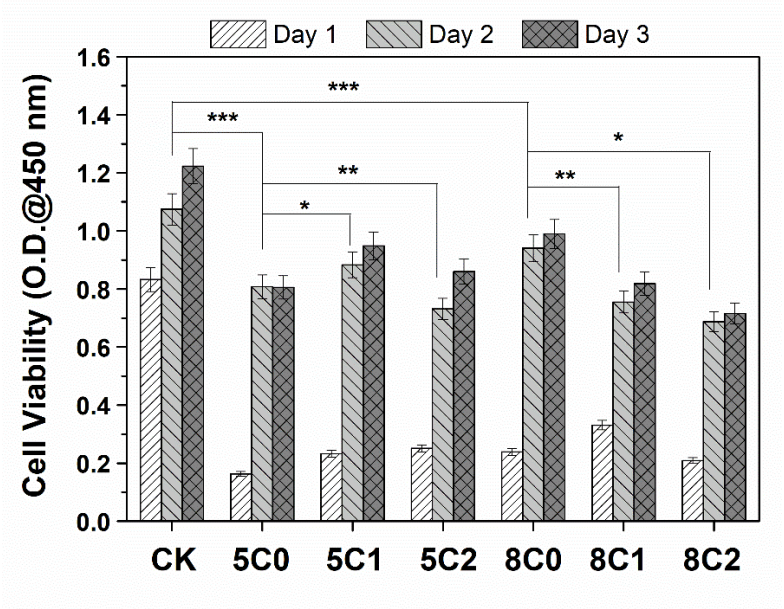

Figure 5. Cytocompatibility of the prepared GC hydrogels evaluated by CCK-8 assay by culturing with NIH 3T3 cells for different days. *$p < 0.05$, **$p < 0.01$, and ***$p < 0.001$.

3.4 In vitro cytocompatibility evaluation

The cytocompatibility of the GC hydrogels was conducted by CCK-8 analysis after seeding NIH 3T3 cells on GC hydrogels and culturing for different days, as shown

in **Fig. 5**. The viability of NIH 3T3 cells cultured on the hydrogels increased from day 1 to day 3, indicating a good cytocompatibility of the prepared GC hydrogels. On day 1, the cell viability on GC hydrogels was lower than that of a control group. However, the cell growth on GC hydrogels was higher on day 2, which might be due to the 3D micro-environment supported by GC hydrogels continuing to support the proliferation of cells. Enhancing the interaction between cells and the extracellular environment is of great importance to engineering functional biomaterial interfaces able to instruct cells with specific commands. On day 1, the cell viability seeded on GC hydrogels without CS-SA was lower than GC hydrogels with CS-SA. Here, it was worth mentioning that SA was introduced to the chitosan to enhance the interactions between cells and biomaterial interfaces based on carbohydrate-carbohydrate interactions suggested as mediators of cell adhesion and aggregation [38, 43, 45].

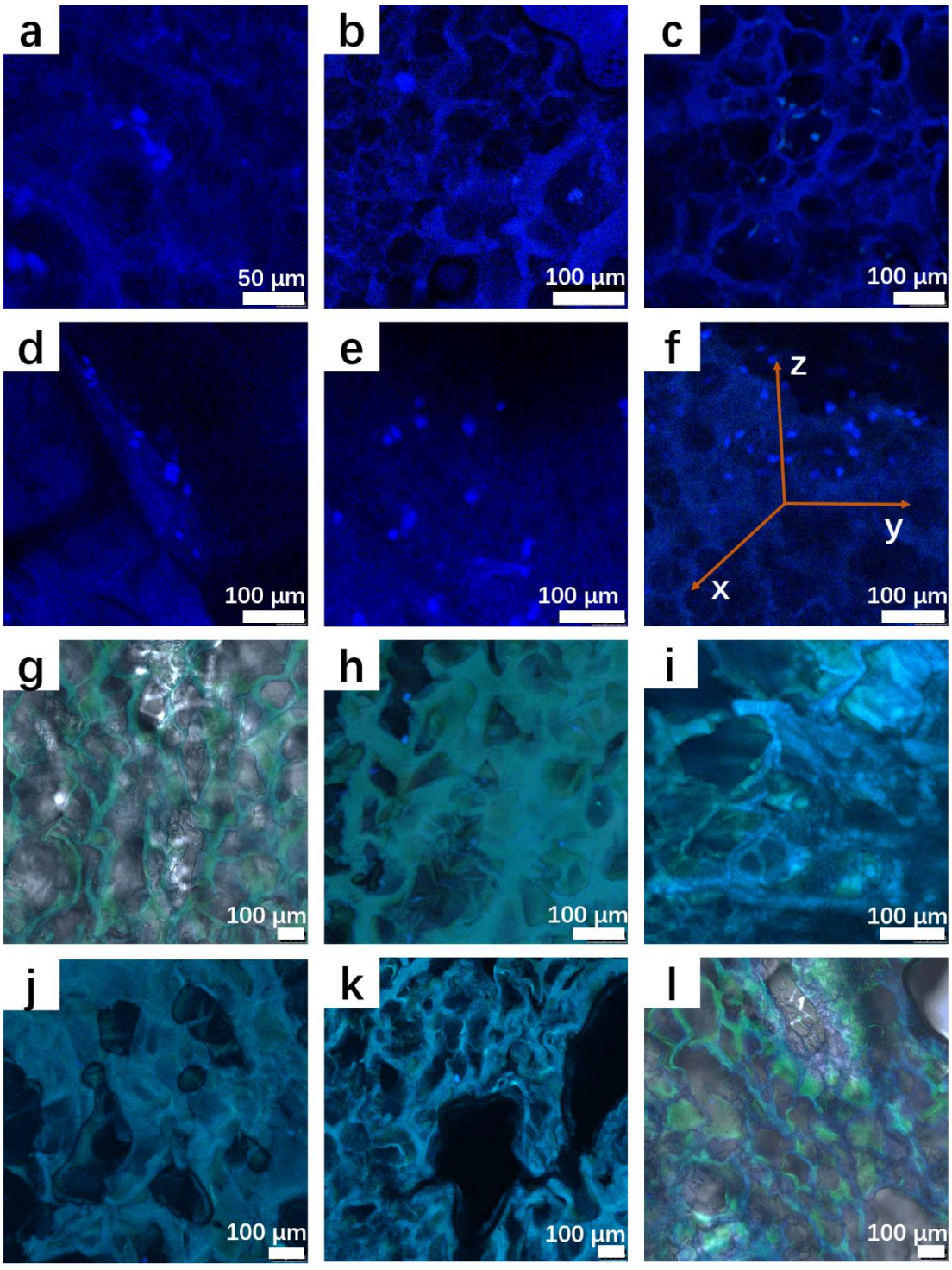

Figure 6. Representative fluorescent microscopy images of GC hydrogels cultured with NIH 3T3 cells for 3 days, the samples were stained using DAPI (a-f) and phalloidin-FITC/DAPI (g-l), respectively. (a, g) 5C0, (b, h) 5C1, (c, i) 5C2, (d, j) 8C0, (e, k) 8C1, and (f, l) 8C2.

On day 3, sample 8C0 displayed the highest O.D value compared to other samples. The hydrogel 8C0 with the highest G-TA concentration possessed the highest crosslinking degree, providing a suitable framework and 3D micro-environment for cell growth. In addition, the NIH 3T3 cells seeded on GC hydrogels on day 3 were evaluated using fluorescent microscopy images (**Fig. 6)**. Interestingly, the framework of the prepared GC hydrogels was stained due to the presence of polysaccharides in the hydrogels [6]. Thus, DAPI and phalloidin-FITC/DAPI were both used respectively to investigate the growth of cells and the microstructure of hydrogels. The porous interconnected structure for all GC hydrogels was observed after the NIH 3T3 cells were seeded and cultured for 3 days, consistent with SEM images of GC hydrogels in a dry state. For samples stained using DAPI alone, some cells could be observed even the framework of hydrogels was stained simultaneously (**Fig. 6a-f**). However, the cells seeded hydrogels were stained using phalloidin-FITC/DAPI, it would be difficult to search cells (**Fig. 6g-l**). With the proliferation of cells on GC hydrogels over days, the cells grew and diffused into the hydrogels; thus, not many cells were observed on the surface of hydrogels. CCK-8 and fluorescent microscopy images confirmed the excellent cytocompatibility of the prepared GC hydrogels.

4. Conclusion

In summary, we have devised an IPN GC hydrogel through the HRP-mediated crosslinking. A series of GC hydrogels based on CS-SA and G-TA with formulated compositions were prepared at physiological temperature. The GC hydrogels with

interconnected structures could provide a suitable 3D microenvironment for cell adhesion and proliferation, confirmed by CCK-8 analysis and fluorescent microscopy images. The results in this paper suggest that these as-prepared enzymatically crosslinked IPN GC hydrogels have great potential as promising biomaterials for biomedical applications.

CRediT authorship contribution statement

Peng Ding: Conceptualization, Methodology, Software, Formal analysis, Writing - original draft, Data curation, Writing - review & editing. **Qianqian Wei:** Methodology, Software. **Ning Tian:** Data curation. **Xiaoyue Ding:** Data curation. **Ling Wang:** Data curation. **Bin Wang:** Data curation. **Oseweuba Valentine Okoro:** Writing - review & editing. **Amin Shavandi:** Conceptualization, Methodology, Writing - review & editing. **Lei Nie:** Conceptualization, Methodology, Software, Formal analysis, Writing - original draft, Writing - review & editing, Supervision.

Acknowledgments

The authors acknowledge support from the Nanhu Scholars Program for Young Scholars of XYNU. The authors acknowledge the help from Prof Lingling Wang, Prof. Qiuju Zhou, Miss Zihe Jin, Dr. Zongwen Zhang, and Dr. Dongli Xu, in the Analysis & Testing Center of XYNU. The authors acknowledge Julia Simińska-Stanny and her PhD transition scholarship from the faculty of engineering (EPB) of the University Libre De Bruxelles (ULB).

Conflicts of Competing Interest

The authors declare no competing financial interest.

References

[1] S. Van Vlierberghe, P. Dubruel, E. Schacht, Biopolymer-based hydrogels as scaffolds for tissue engineering applications: a review, Biomacromolecules, 12 (2011) 1387-1408.
[2] O. Hasturk, K.E. Jordan, J. Choi, D.L. Kaplan, Enzymatically crosslinked silk and silk-gelatin hydrogels with tunable gelation kinetics, mechanical properties and bioactivity for cell culture and encapsulation, Biomaterials, 232 (2020) 119720.
[3] L. Wang, Y. Wu, T. Hu, P.X. Ma, B. Guo, Aligned conductive core-shell biomimetic scaffolds based on nanofiber yarns/hydrogel for enhanced 3D neurite outgrowth alignment and elongation, Acta biomaterialia, 96 (2019) 175-187.
[4] Z. Lei, W. Zhu, X. Zhang, X. Wang, P. Wu, Bio-inspired ionic skin for theranostics, Advanced Functional Materials, 31 (2021) 2008020.
[5] D. Antoni, H. Burckel, E. Josset, G. Noel, Three-dimensional cell culture: a breakthrough in vivo, International journal of molecular sciences, 16 (2015) 5517-5527.
[6] L. Nie, Y. Deng, P. Li, R. Hou, A. Shavandi, S. Yang, Hydroxyethyl Chitosan-Reinforced Polyvinyl Alcohol/Biphasic Calcium Phosphate Hydrogels for Bone Regeneration, Acs Omega, 5 (2020) 10948-10957.
[7] E. Jalalvandi, A. Shavandi, Shear thinning/self-healing hydrogel based on natural polymers with secondary photocrosslinking for biomedical applications, Journal of the Mechanical Behavior of Biomedical Materials, 90 (2019) 191-201.
[8] L. Nie, Q.Y. Wu, H.Y. Long, K.H. Hu, P. Li, C. Wang, M. Sun, J. Dong, X.Y. Wei, J.P. Suo, D.L. Hua, S.L. Liu, H.Y. Yuan, S.F. Yang, Development of chitosan/gelatin hydrogels incorporation of biphasic calcium phosphate nanoparticles for bone tissue engineering, J Biomat Sci-Polym E, 30 (2019) 1636-1657.
[9] L. Nie, D. Chen, Q. Yang, P. Zou, S. Feng, H. Hu, J. Suo, Hydroxyapatite/poly-l-lactide nanocomposites coating improves the adherence and proliferation of human bone mesenchymal stem cells on porous biphasic calcium phosphate scaffolds, Mater Lett, 92 (2013) 25-28.
[10] D. Chen, C.X. Zhang, H.J. Huo, C.C. Ji, M. Sun, L. Nie, Injectable temperature-sensitive hydrogel with VEGF loaded microspheres for vascularization and bone regeneration of femoral head necrosis, Mater Lett, 229 (2018) 138-141.
[11] L. Nie, C. Wang, R. Hou, X. Li, M. Sun, J. Suo, Z. Wang, R. Cai, B. Yin, L. Fang, X. Wei, H. Yuan, Preparation and characterization of dithiol-modified graphene oxide nanosheets reinforced alginate nanocomposite as bone scaffold, SN Applied Sciences, 1 (2019) 545.
[12] X. Wang, S. Tang, S. Chai, P. Wang, J. Qin, W. Pei, H. Bian, Q. Jiang, C. Huang, Preparing printable bacterial cellulose based gelatin gel to promote in vivo bone regeneration, Carbohydrate Polymers, 270 (2021) 118342.

[13] J. Xu, Q. Feng, S. Lin, W. Yuan, R. Li, J. Li, K. Wei, X. Chen, K. Zhang, Y. Yang, Injectable stem cell-laden supramolecular hydrogels enhance in situ osteochondral regeneration via the sustained co-delivery of hydrophilic and hydrophobic chondrogenic molecules, Biomaterials, 210 (2019) 51-61.
[14] Y. Deng, A. Shavandi, O.V. Okoro, L. Nie, Alginate modification via click chemistry for biomedical applications, Carbohydrate Polymers, 270 (2021) 118360.
[15] K. Zheng, Y. Tong, S. Zhang, R. He, L. Xiao, Z. Iqbal, Y. Zhang, J. Gao, L. Zhang, L. Jiang, Flexible Bicolorimetric Polyacrylamide/Chitosan Hydrogels for Smart Real - Time Monitoring and Promotion of Wound Healing, Advanced Functional Materials, 31 (2021) 2102599.
[16] L. Zhou, W. Pi, S. Cheng, Z. Gu, K. Zhang, T. Min, W. Zhang, H. Du, P. Zhang, Y. Wen, Multifunctional DNA Hydrogels with Hydrocolloid-Cotton Structure for Regeneration of Diabetic Infectious Wounds, Advanced Functional Materials, 31 (2021) 2106167.
[17] Y. Fan, M. Lüchow, Y. Zhang, J. Lin, L. Fortuin, S. Mohanty, A. Brauner, M. Malkoch, Nanogel encapsulated hydrogels as advanced wound dressings for the controlled delivery of antibiotics, Advanced Functional Materials, 31 (2021) 2006453.
[18] X. Yin, Y. Hao, Y. Lu, D. Zhang, Y. Zhao, L. Mei, K. Sui, Q. Zhou, J. Hu, Bio-Multifunctional Hydrogel Patches for Repairing Full-Thickness Abdominal Wall Defects, Advanced Functional Materials, 31 (2021) 2105614.
[19] Z. Tu, M. Chen, M. Wang, Z. Shao, X. Jiang, K. Wang, Z. Yao, S. Yang, X. Zhang, W. Gao, Engineering Bioactive M2 Macrophage - Polarized Anti - Inflammatory, Antioxidant, and Antibacterial Scaffolds for Rapid Angiogenesis and Diabetic Wound Repair, Advanced Functional Materials, 31 (2021) 2100924.
[20] S. Guo, M. Yao, D. Zhang, Y. He, R. Chang, Y. Ren, F. Guan, One - Step Synthesis of Multifunctional Chitosan Hydrogel for Full-Thickness Wound Closure and Healing, Advanced Healthcare Materials, 11 (2022) 2101808.
[21] X. Yang, P. Li, W. Tang, S. Du, M. Yu, H. Lu, H. Tan, X. Xing, A facile injectable carbon dot/oxidative polysaccharide hydrogel with potent self-healing and high antibacterial activity, Carbohydrate Polymers, 251 (2021) 117040.
[22] B. Gu, Q. Jiang, B. Luo, C. Liu, J. Ren, X. Wang, X. Wang, A sandwich-like chitosan-based antibacterial nanocomposite film with reduced graphene oxide immobilized silver nanoparticles, Carbohydrate Polymers, 260 (2021) 117835.
[23] X. Peng, X. Xu, Y. Deng, X. Xie, L. Xu, X. Xu, W. Yuan, B. Yang, X. Yang, X. Xia, Ultrafast Self-Gelling and Wet Adhesive Powder for Acute Hemostasis and Wound Healing, Advanced Functional Materials, 31 (2021) 2102583.
[24] C. Choi, S. Kim, C. Cha, Dual-functional alginate crosslinker: Independent control of crosslinking density and cell adhesive properties of hydrogels via separate conjugation pathways, Carbohydrate Polymers, 252 (2021) 117128.
[25] B.-B. Seo, Y. Kwon, J. Kim, K.H. Hong, S.-E. Kim, H.-R. Song, Y.-M. Kim, S.-C. Song, Injectable polymeric nanoparticle hydrogel system for long-term anti-inflammatory effect to treat osteoarthritis, Bioactive materials, 7 (2022) 14-25.
[26] M. Zhu, W. Zhong, W. Cao, Q. Zhang, G. Wu, Chondroinductive/chondroconductive peptides and their-functionalized biomaterials for cartilage tissue engineering, Bioactive materials, 9 (2022) 221-238.
[27] F. Kazemi-Aghdam, V. Jahed, M. Dehghan-Niri, F. Ganji, E. Vasheghani-Farahani, Injectable

chitosan hydrogel embedding modified halloysite nanotubes for bone tissue engineering, Carbohydrate Polymers, 269 (2021) 118311.
[28] K. Yue, X. Li, K. Schrobback, A. Sheikhi, N. Annabi, J. Leijten, W. Zhang, Y.S. Zhang, D.W. Hutmacher, T.J. Klein, Structural analysis of photocrosslinkable methacryloyl-modified protein derivatives, Biomaterials, 139 (2017) 163-171.
[29] Y. Zhang, X. Dou, L. Zhang, H. Wang, T. Zhang, R. Bai, Q. Sun, X. Wang, T. Yu, D. Wu, Facile fabrication of a biocompatible composite gel with sustained release of aspirin for bone regeneration, Bioactive materials, 11 (2022) 130-139.
[30] W. Huang, S. Cheng, X. Wang, Y. Zhang, L. Chen, L. Zhang, Noncompressible Hemostasis and Bone Regeneration Induced by an Absorbable Bioadhesive Self-Healing Hydrogel, Advanced Functional Materials, 31 (2021) 2009189.
[31] S. Yang, J. Zhu, C. Lu, Y. Chai, Z. Cao, J. Lu, Z. Zhang, H. Zhao, Y.-Y. Huang, S. Yao, Aligned fibrin/functionalized self-assembling peptide interpenetrating nanofiber hydrogel presenting multi-cues promotes peripheral nerve functional recovery, Bioactive materials, 8 (2022) 529-544.
[32] R. Boni, A. Ali, A. Shavandi, A.N. Clarkson, Current and novel polymeric biomaterials for neural tissue engineering, Journal of Biomedical Science, 25 (2018) 90.
[33] Y. Zhang, S. Liu, T. Li, L. Zhang, U. Azhar, J. Ma, C. Zhai, C. Zong, S. Zhang, Cytocompatible and non-fouling zwitterionic hyaluronic acid-based hydrogels using thiol-ene “click” chemistry for cell encapsulation, Carbohydrate Polymers, 236 (2020) 116021.
[34] E. Jalalvandi, A. Shavandi, In situ-forming and pH-responsive hydrogel based on chitosan for vaginal delivery of therapeutic agents, Journal of Materials Science: Materials in Medicine, 29 (2018) 158.
[35] H.Y. Jung, P. Le Thi, K.-H. HwangBo, J.W. Bae, K.D. Park, Tunable and high tissue adhesive properties of injectable chitosan based hydrogels through polymer architecture modulation, Carbohydrate Polymers, 261 (2021) 117810.
[36] R.D. Cummings, J.M. Pierce, The challenge and promise of glycomics, Chemistry & biology, 21 (2014) 1-15.
[37] K. Handa, S.-i. Hakomori, Carbohydrate to carbohydrate interaction in development process and cancer progression, Glycoconjugate journal, 29 (2012) 627-637.
[38] B.r. Lorenz, L. Álvarez de Cienfuegos, M. Oelkers, E. Kriemen, C. Brand, M. Stephan, E. Sunnick, D. Yu¨ksel, V. Kalsani, K. Kumar, Model system for cell adhesion mediated by weak carbohydrate–carbohydrate interactions, Journal of the American Chemical Society, 134 (2012) 3326-3329.
[39] S. Hakomori, Carbohydrate-to-carbohydrate interaction, through glycosynapse, as a basis of cell recognition and membrane organization, Glycoconjugate Journal, 21 (2004) 125-137.
[40] L. Ding, W. Cheng, X. Wang, S. Ding, H. Ju, Carbohydrate Monolayer Strategy for Electrochemical Assay of Cell Surface Carbohydrate, Journal of the American Chemical Society, 130 (2008) 7224-7225.
[41] N. Kojima, B.A. Fenderson, M.R. Stroud, R.I. Goldberg, R. Habermann, T. Toyokuni, S.-I. Hakomori, Further studies on cell adhesion based on Lex-Lex interaction, with new approaches: embryoglycan aggregation of F9 teratocarcinoma cells, and adhesion of various tumour cells based on Lex expression, Glycoconjugate Journal, 11 (1994) 238-248.
[42] X. Fernàndez-Busquets, M.M. Burger, Circular proteoglycans from sponges: first members of the spongican family, Cellular and Molecular Life Sciences CMLS, 60 (2003) 88-112.
[43] X. Li, Y. Xiong, G. Qing, G. Jiang, X. Li, T. Sun, X. Liang, Bioinspired Saccharide–Saccharide

Interaction and Smart Polymer for Specific Enrichment of Sialylated Glycopeptides, ACS Applied Materials & Interfaces, 8 (2016) 13294-13302.
[44] G. Qing, X. Li, P. Xiong, C. Chen, M. Zhan, X. Liang, T. Sun, Dipeptide-Based Carbohydrate Receptors and Polymers for Glycopeptide Enrichment and Glycan Discrimination, ACS Applied Materials & Interfaces, 8 (2016) 22084-22092.
[45] Y. Xiong, M. Li, Q. Lu, G. Qing, T. Sun, Sialic Acid-Targeted Biointerface Materials and Bio-Applications, Polymers, 9 (2017) 249.
[46] A.P. Dhand, J.H. Galarraga, J.A. Burdick, Enhancing Biopolymer Hydrogel Functionality through Interpenetrating Networks, Trends in Biotechnology, 39 (2021) 519-538.
[47] N.R. Raia, B.P. Partlow, M. McGill, E.P. Kimmerling, C.E. Ghezzi, D.L. Kaplan, Enzymatically crosslinked silk-hyaluronic acid hydrogels, Biomaterials, 131 (2017) 58-67.
[48] H. Sashiwa, Y. Makimura, Y. Shigemasa, R. Roy, Chemical modification of chitosan: preparation of chitosan–sialic acid branched polysaccharide hybrids, Chemical Communications, (2000) 909-910.
[49] M. Vahdati, G. Ducouret, C. Creton, D. Hourdet, Topology-Specific Injectable Sticky Hydrogels, Macromolecules, 53 (2020) 9779-9792.
[50] H. El Knidri, R. Belaabed, A. Addaou, A. Laajeb, A. Lahsini, Extraction, chemical modification and characterization of chitin and chitosan, Int J Biol Macromol, 120 (2018) 1181-1189.
[51] L. Nie, P. Zou, S. Feng, J. Suo, Temperature-sensitive star-shaped block copolymers hydrogels for an injection application: Phase transition behavior and biocompatibility, Journal of Materials Science: Materials in Medicine, 24 (2013) 689-700.
[52] P. Zou, J. Suo, L. Nie, S. Feng, Temperature-sensitive biodegradable mixed star-shaped block copolymers hydrogels for an injection application, Polymer, 53 (2012) 1245-1257.
[53] Z. Wang, Y. Zhang, Y. Yin, J. Liu, P. Li, Y. Zhao, D. Bai, H. Zhao, X. Han, Q. Chen, High-Strength and Injectable Supramolecular Hydrogel Self-Assembled by Monomeric Nucleoside for Tooth-Extraction Wound Healing, Adv Mater, 34 (2022) e2108300.
[54] E.S. Dragan, Design and applications of interpenetrating polymer network hydrogels. A review, Chemical Engineering Journal, 243 (2014) 572-590.
[55] A.H. Karoyo, L.D. Wilson, A Review on the Design and Hydration Properties of Natural Polymer-Based Hydrogels, Materials, 14 (2021).
[56] S. Liu, Y. Zhao, H. Wei, L. Nie, P. Ding, H. Sun, Y. Guo, T. Chen, O.V. Okoro, A. Shavandi, L. Fan, Injectable hydrogels based on silk fibroin peptide grafted hydroxypropyl chitosan and oxidized microcrystalline cellulose for scarless wound healing, Colloids and Surfaces A: Physicochemical and Engineering Aspects, (2022) 129062.